



## Improved radiosynthesis of the apoptosis marker $^{18}\text{F}$ -ICMT11 including biological evaluation

Matthias Glaser<sup>a,\*</sup>, Julian Goggi<sup>b,†</sup>, Graham Smith<sup>c</sup>, Matthew Morrison<sup>b</sup>, Sajinder K. Luthra<sup>a</sup>, Edward Robins<sup>a,†</sup>, Eric O. Aboagye<sup>c</sup>

<sup>a</sup> MDx Discovery (Part of GE Healthcare), Hammersmith Imanet Ltd, Hammersmith Hospital, Du Cane Road, London W12 0NN, United Kingdom

<sup>b</sup> MDx Discovery (Part of GE Healthcare), The Grove Centre, White Lion Road, Amersham HP7 9LL, United Kingdom

<sup>c</sup> Comprehensive Cancer Imaging Centre, Faculty of Medicine, Imperial College London, Hammersmith Hospital, Du Cane Road, London W12 0NN, United Kingdom

### ARTICLE INFO

#### Article history:

Received 25 August 2011

Revised 29 September 2011

Accepted 3 October 2011

Available online 8 October 2011

#### Keywords:

Apoptosis

PET

Isatin

Caspase

Fluorine-18

Click chemistry

### ABSTRACT

We improved the specific radioactivity of the apoptosis imaging isatin derivative  $^{18}\text{F}$ -ICMT11. We then evaluated  $^{18}\text{F}$ -ICMT11 in EL4 tumor-bearing mice 24 h after treatment with etoposide/cyclophosphamide combination therapy. Dynamic PET imaging demonstrated increased uptake in the drug-treated ( $0.115 \pm 0.011$  SUV) compared to the vehicle-treated EL4 tumors ( $0.083 \pm 0.008$  SUV). This effect correlated to the observed increases in apoptotic index.

© 2011 Elsevier Ltd. All rights reserved.

Apoptosis – programmed cell death – can be triggered both by intrinsic and extrinsic cell signals and is fundamental to the mechanism of action of current cancer treatments.<sup>1</sup> Ideally, a noninvasive molecular imaging agent that targets apoptosis should be able to monitor early tumor response to classical anti-cancer therapy. This would then support further decisions on treatment options for patients. An apoptosis tracer would be also beneficial in preclinical development of novel chemotherapeutic agents.

So far, various avenues have been explored to investigate apoptosis in the living organism. A good overview of the field can be gathered from several well-written review articles.<sup>1–4</sup> Numerous studies have been dedicated to annexin-V, a calcium dependent phosphatidyl serine (PS) binding protein of 32–36 kDa.<sup>3</sup> The technetium-99 m labelled annexin-V probe is probably the most advanced clinical apoptosis tracer for single photon computed tomography (SPECT). Annexin-V has been also conjugated with PET radionuclides such as  $^{18}\text{F}$  and  $^{124}\text{I}$ .<sup>5–16</sup> There are however known limitations to this vector protein. The radiotracer is not necessarily able to differentiate between necrosis and apoptosis as in both cases PS residues are exposed.<sup>17,18</sup> Recent data from a mouse breast tumor model pointed to potential problems of  $^{99\text{m}}\text{Tc}$ -annexin-V indicating absence of an

association with immunohistochemical measures of apoptosis.<sup>19</sup> In addition, there are indications that the apoptotic display of PS can be reversible<sup>20</sup> and can also occur during myotube formation.<sup>21</sup> Imaging anionic phospholipids via radiolabelled  $\gamma$ -carboxyglutamic acid (Gla),<sup>22</sup> duramycin,<sup>23</sup> or small peptide-based radiotracers<sup>24</sup> have been suggested as an alternative approaches. However, it appears likely that some of the above mentioned limitations of annexin-V still apply.

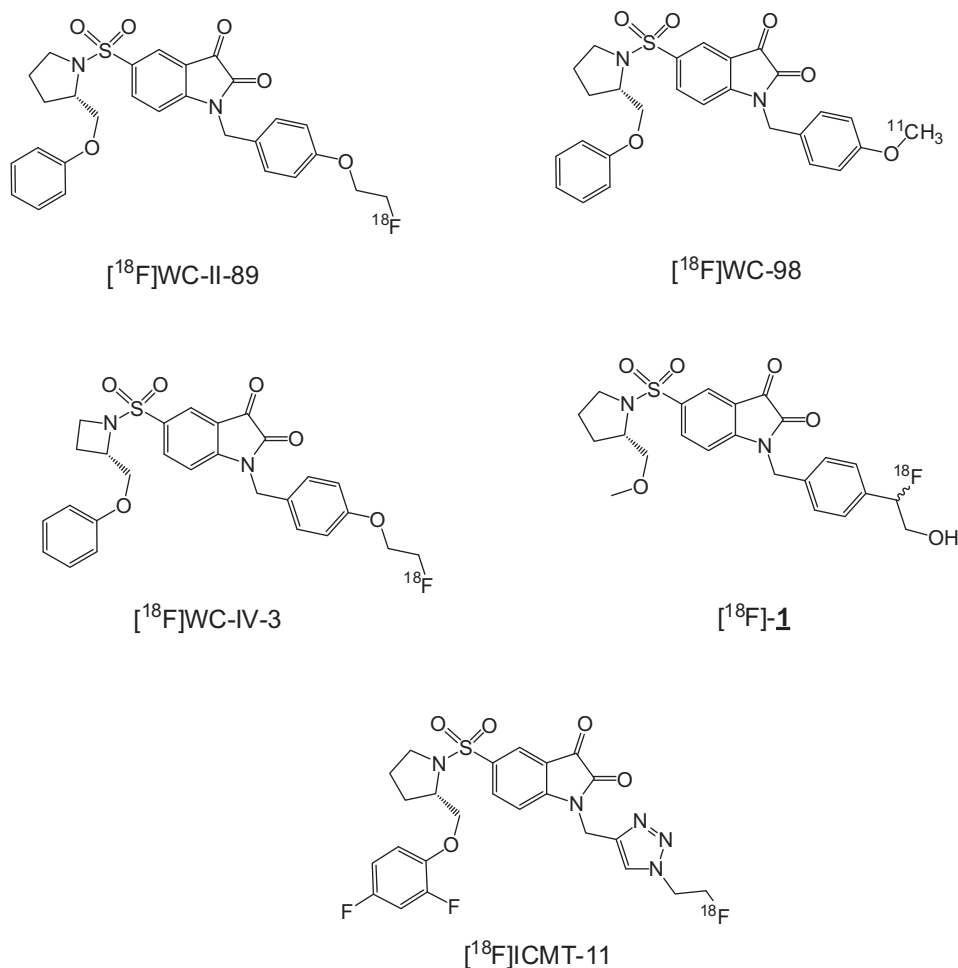
Imaging of cysteine aspartate-specific protease (caspase) activity in the apoptotic signaling pathway has been identified as an alternative target to visualize cell death. A number of 5-pyrrolidinylsulfonyl isatin derivatives were confirmed to bind with high affinity to the most relevant executioner caspase-3.<sup>25</sup> These compounds demonstrated better cell permeability compared to the Z-VAD-fmk peptide<sup>26</sup> to reach activated caspase.

Figure 1 shows the structures of published  $^{18}\text{F}/^{11}\text{C}$  labelled isatin compounds  $^{18}\text{F}$ -WC-II-89,<sup>27</sup>  $^{18}\text{F}$ -WC-IV-3,<sup>28</sup>  $^{18}\text{F}$ -WC-98,<sup>28</sup> and  $^{18}\text{F}$ -1.<sup>29</sup> We recently reported a Click chemistry strategy to synthesize  $^{18}\text{F}$ -ICMT11.<sup>30</sup> This approach avoided protection of the reactive dicarbonyl function. However, that process gave rise to a stable by-product which could not be removed from the  $^{18}\text{F}$  tracer. Since this material might potentially compete in the caspase-3 binding, we undertook further optimization of the radiochemistry protocol to address that issue. We also investigated the in vivo behavior of  $^{18}\text{F}$ -ICMT11 – as prepared by the new protocol – in the murine lymphoma xenograft EL4 model.<sup>31</sup>

\* Corresponding author. Tel.: +44 149 454 6121; fax +44 149 454 3284.

E-mail address: [matthias.glaser@ge.com](mailto:matthias.glaser@ge.com) (M. Glaser).

† Present address: Singapore Biolmaging Consortium, HELIOS, 11 Biopolis Way, Singapore 138667, Singapore.



**Figure 1.** Structures of isatin analogs labelled with positron emitters.

<sup>18</sup>F-ICMT11 has been prepared for the initial in vivo study following the original radiochemistry protocol.<sup>30</sup> The estimated specific radioactivity, impurity level and radiochemical yields are given in Table 1 (further information on the radiochemical methods can be found in the Supplementary data). The protocol could be significantly improved by introducing bathophenanthroline disulfonic acid disodium ligand (BPDS) as an additive to stabilize the Cu(I) catalyst (Route A, Scheme 1). We found that BPDS helped both to reduce the amount of required alkyne precursor **2** (1 mg vs 3 mg), and also to shorten the reaction time (15 min vs 30 min). The resulting formulated <sup>18</sup>F-ICMT11 showed a reduced carrier

level (Table 1). While our study was in progress, other investigators also discovered that BPDS accelerates the kinetics of the cycloaddition.<sup>32,33</sup>

The radiosynthesis of <sup>18</sup>F-ICMT11 following Route A gave rise to a stable by-product of almost identical HPLC retention time as the radioactive product. It was possible to isolate a small quantity of that material (<100 µg). However, MS and <sup>1</sup>H NMR data were not conclusive. Accurate MALDI-TOF and ESI MS suggested two species (see Supplementary data, Fig. 4). The UV spectrum of the material revealed a profile similar to the stable <sup>18</sup>F-ICMT11 reference sample. For this reason, it appeared particularly important to keep the

**Table 1**  
Comparison of specific radioactivities and radiochemical yields of <sup>18</sup>F-ICMT11.

Route	Method	Specific Radioactivity <sup>a</sup> (GBq/µmol)	Amount of stable product <sup>a</sup> (µg/mL)	EOS RCY <sup>b</sup>
A	Literature <sup>30</sup>	1.2 (1)	13.8 (1)	3.4 ± 1.5% (5)
A	I <sup>c,d</sup>	7.0 ± 5.6 (5)	4.6 ± 4.3 (5)	3.2 ± 0.8% (5)
B	II <sup>c,e</sup>	13.3 ± 4.4 (3)	4.8 ± 3.4 (3)	3 ± 1% (3)
B	III <sup>c,f</sup>	17 ± 3 (3)	1.6 ± 0.9 (3)	1% (2)
B	IV <sup>c,g</sup>	24 ± 19 (3)	4.1 ± 4.1 (3)	3.0 ± 2.6% (3)

The number of experiments is given in brackets.

<sup>a</sup> Estimated, based on isatin-like stable by-product.

<sup>b</sup> End of synthesis radiochemical yield of formulated product, nondecay corrected, referring to [<sup>18</sup>F]-fluoride.

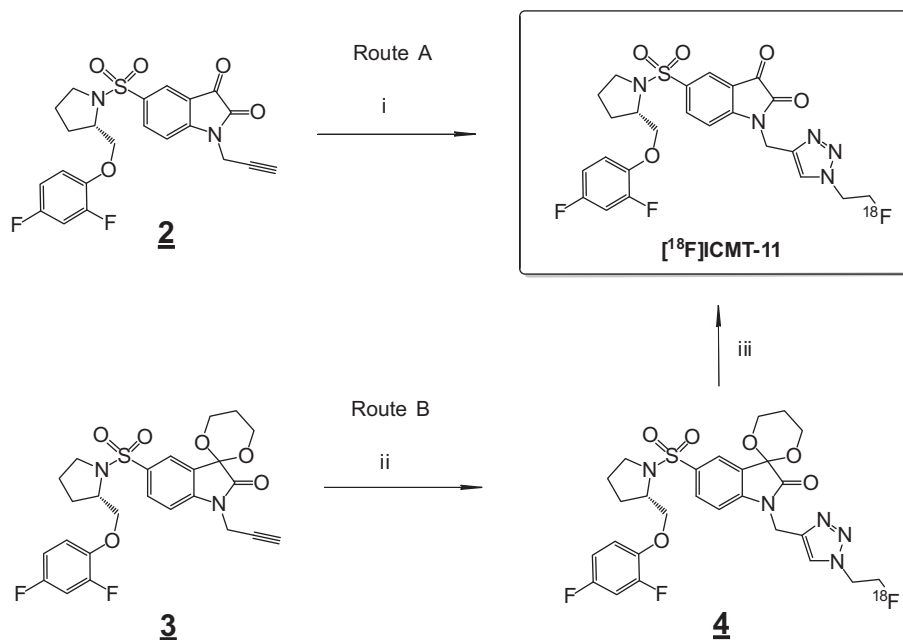
<sup>c</sup> Using BPDS in the cycloaddition step.

<sup>d</sup> Using isatin precursor **2**, without carbonyl protecting group.

<sup>e</sup> HCl/microwave deprotection of intermediate **4**.

<sup>f</sup> H<sub>2</sub>SO<sub>4</sub> deprotection of intermediate **4**.

<sup>g</sup> C18-SepPak purification prior to H<sub>2</sub>SO<sub>4</sub> deprotection of intermediate **4**.



**Scheme 1.** Preparation of  $^{18}\text{F}$ -ICMT11. (i) 2- $^{18}\text{F}$ fluoroethylazide,  $\text{CuSO}_4/\text{Na}$ -ascorbate, pH 5.0, BPDS, 30 min rt, preparative HPLC; (ii) 2- $^{18}\text{F}$ fluoroethylazide,  $\text{CuSO}_4/\text{Na}$ -ascorbate, pH 5.0, BPDS, 15 min rt; (iii) 6 N HCl, microwave ( $3 \times 2\text{s}$  @ 50 W), preparative HPLC.

level of by-product as low as possible in order to avoid a potential caspase-3/7 blocking.

From studies with model isatin compounds we concluded that the level of stable impurity did not depend on the presence of the sulfonamide moiety. Also, protecting a sulfonamide-free model isatin with a cyclic acetal<sup>34</sup> suppressed the impurity (data not shown). Therefore, we prepared an acetal protected isatin alkyne precursor **3** for the Click labelling chemistry (Route B). The resulting intermediate **4** was formed in quantitative radiochemical yields. The deprotection was achieved by using both microwave heating (HCl additive, Method II, used to prepare samples for biology study) or conventional heating ( $\text{H}_2\text{SO}_4$  additive, Method III).

The experimental results revealed that the radiosynthesis of  $^{18}\text{F}$ -ICMT11 had been improved with regard to labelling efficiency. However, the improvements in the specific radioactivity from Routes A and B were somewhat lower than anticipated. It appeared that any isatin alkyne **2** – either as nonprotected precursor or in situ formed upon acidic deprotection – would react with  $\text{Cu(I)}$  species to form the unwanted carrier material. Therefore an experiment was designed to investigate the removal of  $\text{Cu(I)}$  prior to deprotection in Route B (Method IV). However, the by-product was still observed, albeit to a lesser extent. This finding suggested that the by-product formation was either independent of copper catalysis or the pre-deprotection purification was inefficient in removing reactive copper species.

Finally, a promising one-pot approach was investigated with the aim to increase the overall radiochemical yield and to simplify the process (Method V). Here,  $^{18}\text{F}$ -ICMT11 was prepared in the same vial that was used to produce 2- $^{18}\text{F}$ fluoroethylazide. Without distillation of 2- $^{18}\text{F}$ fluoroethylazide,  $^{18}\text{F}$ -ICMT11 could be obtained using copper wire as  $\text{Cu(I)}$  source. The analytical data are shown in the Supplementary data. However, the protocol was not further developed.

The biology studies described here were performed in order to investigate the performance of  $^{18}\text{F}$ -ICMT11 for imaging combination etoposide and cyclophosphamide therapy-induced apoptosis in an EL-4 (murine lymphoma) tumor model in vivo using PET. The isatin compound  $^{18}\text{F}$ -ICMT11 has been previously evaluated for cyclophosphamide-induced tumor apoptosis in 38C13 murine

lymphoma.<sup>35</sup> That study found up to twofold increased tumor binding after drug treatment.

Literature studies have shown that a murine lymphoma (EL4) tumor model undergoes large-scale apoptosis following treatment with etoposide.<sup>31,36</sup> EL4 cells form a solid tumor when implanted subcutaneously into C57/BL6 mice and readily undergo apoptosis in vivo when exposed to chemotherapeutic agents. It has been demonstrated that treatment of tumor bearing mice with a combination of cyclophosphamide and etoposide for 48 h show an increase in the average levels of apoptosis in EL4 tumors from basal levels of 4% to 32%.<sup>31</sup> The distribution of apoptosis was heterogenous, with regions of some tumor sections containing large numbers of apoptotic cells.<sup>31</sup> Additional in-house validation studies confirmed that a similar level of apoptosis can be seen 20–24 h post therapy in the EL4 tumor model (see Supplementary data, Table 1). Additionally, use of animals 24 h post treatment was logistically and ethically preferred to using animals at the 48 h time point. Therefore, 24 h was chosen

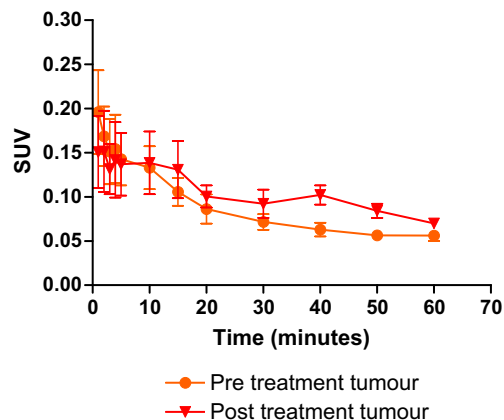


**Figure 2.** Summary of imaging data of the lower specific activity compound  $^{18}\text{F}$ -ICMT11 in the EL4 model. Data expressed dynamically prior to treatment and post treatment with combined etoposide and cyclophosphamide therapy (SUV  $\pm$  SD,  $n = 5$  pre-treatment \*one animal data omitted due to reconstruction issues,  $n = 3$  post treatment).

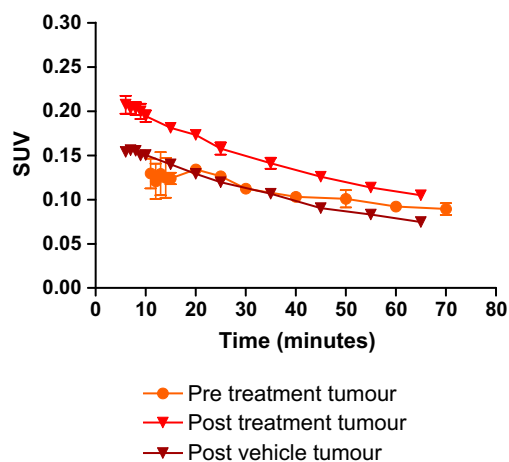


**Figure 3.** Summary of imaging data of the high specific activity compound  $^{18}\text{F}$ -ICMT11-hsp in the EL4 model. Data expressed dynamically prior to treatment ( $n = 3$ ) and post treatment with either vehicle ( $n = 1$ ) or combined etoposide and cyclophosphamide therapy ( $n = 2$ ) (SUV  $\pm$  SD).

as the optimum timepoint for apoptosis post administration of etoposide/cyclophosphamide.

Here, the acquired  $^{18}\text{F}$ -ICMT11 images demonstrate uptake into EL4 tumors pre-treatment of  $0.058 \pm 0.013$  SUV at 40–60 min post injection, see Figure 2. Twenty-four hours following vehicle treatment, the uptake into the vehicle treated tumors was similar ( $0.048 \pm 0.015$  SUV at 40–60 min p.i.), whereas 24 h after anti-cancer treatment (combined etoposide and cyclophosphamide therapy) the uptake into the treated tumors was significantly increased to  $0.085 \pm 0.019$  SUV at 40–60 min p.i. see Supplementary data, Table 2, for full details).

These results demonstrate that tumor uptake was significantly different in the murine tumors pre and post therapy, indicating that changes in the level of apoptosis post therapy can be detected using the imaging agent  $^{18}\text{F}$ -ICMT11. For comparison, region of interest (ROI) analysis of skeletal muscle demonstrated that uptake was equivalent pre and post therapy ( $0.122 \pm 0.07$  SUV and  $0.138 \pm 0.11$  SUV).

In order to assess the utility of the high specific activity compound,  $^{18}\text{F}$ -ICMT11-hsp, radiotracer uptake was measured using positron emission tomography in the same EL4 tumor bearing animals before treatment and following treatment with a combination of etoposide (67 mg/kg) and cyclophosphamide (100 mg/kg). The acquired  $^{18}\text{F}$ -ICMT11-hsp images demonstrated uptake into EL4 tumors pre-treatment of  $0.094 \pm 0.009$  SUV at 40–60 min post injection, see Figure 3. Twenty-four hours following vehicle treatment, the uptake into the vehicle treated tumors was not statistically different ( $0.083 \pm 0.008$  SUV at 40–60 min p.i.), whereas 24 h after anti-cancer treatment (combined etoposide and cyclophosphamide therapy) the uptake into the treated tumors was significantly increased to  $0.115 \pm 0.011$  SUV at 40–60 min p.i. see Supplementary data, Table 2, for full details).

These results demonstrate that tumor uptake was significantly different in the murine tumors pre and post anti-cancer therapy, signifying that changes in the level of apoptosis post therapy can be detected using the imaging agent  $^{18}\text{F}$ -ICMT11. For comparison, region of interest (ROI) analysis of skeletal muscle showed that uptake was equivalent pre and post therapy ( $0.148 \pm 0.022$  SUV and  $0.179 \pm 0.035$  SUV).

Apoptosis levels within the context of activated caspase-3 were verified in treated animals using the Caspase Glo assay (Fig. 4 and Supplementary data).

In summary, we described here experimental improvements for the radiochemical preparation of  $^{18}\text{F}$ -ICMT11. Introduction of a

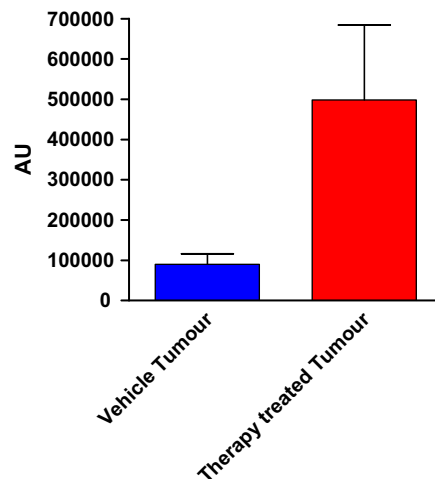


**Figure 4.** Apoptosis levels (arbitrary units: assessed using the Glo assay for activated caspase 3) in tumors treated with vehicle or tumor treated with anti-cancer therapy (combination of etoposide and cyclophosphamide) displaying significantly increased levels of caspase-3 in the drug treated tumors.

BPDS additive increased the labelling efficiency of the 2- $^{18}\text{F}$ fluoroethylazide cycloaddition step. Acetal protection of the reactive isatin carbonyl group during that reaction did not completely suppress the formation of a stable by-product.

The data presented here demonstrated that the EL4 therapy model was suitable for imaging apoptosis and assessment of both  $^{18}\text{F}$ -ICMT11 and  $^{18}\text{F}$ -ICMT11-hsp.

Dynamic imaging over a 1 h period with both  $^{18}\text{F}$ -ICMT11 and  $^{18}\text{F}$ -ICMT11-hsp in the EL4 tumor model pre and post therapy (intra animal longitudinal imaging studies) was successfully accomplished. Overall, the dynamic time versus radioactivity data showed significantly improved uptake in the treated versus non-treated EL4 tumors that was associated with the observed increases in apoptotic index as determined using the Caspase Glo assay (for details see Supplementary data).

The conclusion from this series of imaging studies is that  $^{18}\text{F}$ -ICMT11 shows promise as a PET agent to measure the levels of apoptosis in treated tumors. The improved specific activity compound  $^{18}\text{F}$ -ICMT11-hsp displayed marginally higher tumor retention than the lower specific activity compound  $^{18}\text{F}$ -ICMT11 with no significant difference in uptake observed in the reference tissue, skeletal muscle.

#### Supplementary data

Supplementary data associated with this article can be found, in the online version, at doi:10.1016/j.bmcl.2011.10.001.

#### References and notes

- Niu, G.; Chen, X. *J. Nucl. Med.* **2010**, *51*, 1659.
- Blankenberg, F. G. *J. Nucl. Med.* **2008**, *49*, 815.
- Zhao, M. *Anti-Cancer Agents Med. Chem.* **2009**, *9*, 1018.
- Lahorte, C. M. M.; Vanderheyden, J.-L.; Steinmetz, N.; Wiele, C. V. D.; Dierckx, R. A.; Slegers, G. *Eur. J. Nucl. Med. Biol. Imaging* **2004**, *31*, 887.
- Zijlstra, S.; Gunawan, J.; Burchert, W. *Appl. Radiat. Isot.* **2003**, *58*, 201.
- Grierson, J. R.; Yagle, K. J.; Eary, J. F.; Tait, J. F.; Gibson, D. F.; Lewellen, B.; Link, J. M.; Krohn, K. A. *Bioconjugate Chem.* **2004**, *15*, 373.
- Murakami, Y.; Takamatsu, H.; Taki, J.; Tatsumi, M.; Noda, A.; Ichise, R.; Tait, J. F.; Nishimura, S. *Eur. J. Nucl. Med. Mol. Imaging* **2004**, *31*, 469.
- Toretsky, J.; Levenson, A.; Weinberg, I. N.; Tait, J. F.; Üren, A.; Mease, R. C. *Nucl. Med. Biol.* **2004**, *31*, 747.
- Yagle, K. J.; Eary, J. F.; Tait, J. F.; Grierson, J. R.; Link, J. M.; Lewellen, B.; Gibson, D. F.; Krohn, K. A. *J. Nucl. Med.* **2005**, *46*, 658.
- Li, X. H.; Link, J. M.; Stekhova, S.; Yagle, K. J.; Smito, C.; Krohn, K. A.; Tait, J. F. *Bioconjugate Chem.* **2008**, *19*, 1684.

11. Keen, H.; Dekker, B. A.; Disley, L.; Hastings, D.; Lyons, S.; Reader, A. J.; Ottewell, P.; Watson, A.; Zweit, J. *Nucl. Med. Biol.* **2005**, *32*, 395.
12. Dekker, B.; Keen, H.; Shaw, D.; Disley, L.; Hastings, D.; Hadfield, J.; Reader, A.; Allan, D.; Julyan, P.; Watson, A.; Zweit, J. *Nucl. Med. Biol.* **2005**, *32*, 403.
13. Dekker, B.; Keen, H.; Lyons, S.; Disley, L.; Hastings, D.; Reader, A. J.; Ottewell, P.; Watson, A.; Zweit, J. *Nucl. Med. Biol.* **2005**, *32*, 241.
14. Glaser, M.; Collingridge, D. R.; Aboagye, E. O.; Bouchier-Hayes, L.; Hutchinson, O. C.; Martin, S. J.; Price, P.; Brady, F.; Luthra, S. K. *Appl. Radiat. Isot.* **2003**, *58*, 55.
15. Collingridge, D. R.; Glaser, M.; Osman, S.; Barthel, H.; Hutchinson, O. C.; Luthra, S. K.; Brady, F.; Bouchier-Hayes, L.; Martin, S. J.; Workman, P.; Aboagye, E. O. *Br. J. Cancer* **2003**, *89*, 1327.
16. Glaser, M.; Collingridge, D. R.; Aboagye, E. O.; Bouchier-Hayes, L.; Brown, D. J.; Hutchinson, O. C.; Martin, S.; Price, P.; Luthra, S. K.; Brady, F. *J. Labelled Compd. Radiopharm.* **2001**, *44*, S336.
17. Van De Wiele, C.; Lahorte, C.; Vermeersch, H.; Loose, D.; Mervillie, K.; Steinmetz, N. D.; Vanderheyden, J. L.; Cuvelier, C. A.; Slegers, G.; Dierck, R. A. *J. Clin. Oncol.* **2003**, *21*, 3483.
18. Krysko, O.; De Ridder, L.; Cornelissen, M. *Apoptosis* **2004**, *9*, 495.
19. Beekman, C. A. C.; Buckle, T.; van Leeuwen, A. C.; Valdes Olmos, R. A.; Verheij, M.; Rottenberg, S.; Van Leeuwen, F. W. B. *Appl. Radiat. Isot.* **2011**, *69*, 656.
20. Hammill, A. K.; Uhr, J. W.; Scheuermann, R. H. *Exp. Cell Res.* **1999**, *251*, 16.
21. Van den Eijnde, S. M.; Van den Hoff, M. J. B.; Reutelingsperger, C. P. M.; Van Heerde, W. L.; Henfling, M. E. R.; Vermeij-Keers, C.; Schutte, B.; Borgers, M.; Ramaekers, F. C. S. *J. Cell Sci.* **2001**, *114*, 3631.
22. Cohen, A.; Shirvan, A.; Levin, G.; Grimberg, H.; Reshef, A.; Ziv, I. *Cell Res.* **2009**, *19*, 625.
23. Zhao, M.; Li, Z. X.; Bugenhagen, S. J. *Nucl. Med.* **2008**, *49*, 1345.
24. Xiong, C.; Brewer, K.; Song, S.; Zhang, R.; Lu, W.; Wen, X.; Li, C. *J. Med. Chem.* **2011**, *54*, 1825.
25. Kopka, K.; Faust, A.; Keul, P.; Wagner, S.; Breyholz, H. J.; Holtke, C.; Schober, O.; Schafers, M.; Levkau, B. *J. Med. Chem.* **2006**, *49*, 6704.
26. Haberkorn, U.; Kinscherf, R.; Krammer, P. H.; Mier, W.; Eisenhut, M. *Nucl. Med. Biol.* **2001**, *28*, 793.
27. Zhou, D.; Chu, W.; Rothfuss, J.; Zeng, C.; Xu, J.; Jones, L.; Welch, M. J.; Mach, R. H. *Bioorg. Med. Chem. Lett.* **2006**, *16*, 5041.
28. Chen, D. L.; Zhou, D.; Chu, W. H.; Herrbrich, P. E.; Jones, L. A.; Rothfuss, J. M.; Engle, J. T.; Geraci, M.; Welch, M. J.; Mach, R. H. *Nucl. Med. Biol.* **2009**, *36*, 651.
29. Podichetty, A. K.; Wagner, S.; Schroer, S.; Faust, A.; Schafers, M.; Schober, O.; Kopka, K.; Haufe, G. *J. Med. Chem.* **2009**, *52*, 3484.
30. Smith, G.; Glaser, M.; Perumal, M.; Nguyen, Q.-D.; Shan, B.; Årstad, E.; Aboagye, E. O. *J. Med. Chem.* **2008**, *51*, 8057.
31. Zhao, M.; Beauregard, D. A.; Loizou, L.; Davletov, B.; Brindle, K. M. *Nat. Med.* **2001**, *7*, 1241.
32. Devaraj, N. K.; Keliher, E.; Thurber, G. M.; Nahrendorf, M.; Weissleder, R. *Bioconjugate Chem.* **2009**, *20*, 397.
33. Gill, H. S.; Tinianow, J. N.; Ogasawara, A.; Flores, J. E.; Vanderbilt, A. N.; Raab, H.; Scheer, J. M.; Vandlen, R.; Williains, S. P.; Marik, J. *J. Med. Chem.* **2009**, *52*, 5816.
34. Zhou, D.; Chu, W. H.; Chen, D. L.; Wang, Q.; Reichert, D. E.; Rothfuss, J.; D'Avignon, A.; Welch, M. J.; Mach, R. H. *Org. Biomol. Chem.* **2009**, *7*, 1337.
35. Nguyen, Q. D.; Smith, G.; Glaser, M.; Perumal, M.; Årstad, E.; Aboagye, E. O. *Proc. Natl. Acad. Sci. U.S.A.* **2009**, *106*, 16375.
36. Schmitz, J. E.; Kettunen, M. I.; Hu, D. E.; Brindle, K. M. *Magn. Reson. Med.* **2005**, *54*, 43.